Comparison of Globally Complete Versions of GPCP and

CMAP Monthly Precipitation Analyses

by

Scott Curtis (1)

and

Robert Adler (2), George Huffman (3)

(1) JCET University of Maryland Baltimore County
(2) NASA/GSFC Laboratory for Atmospheres
(3) Science Systems and Applications, Inc.

Abstract

In this study two global observational precipitation products, namely the Global Precipitation Climatology Project's (GPCP) community data set and CPC's Merged Analysis of Precipitation (CMAP), are compared on global to regional scales in the context of the different satellite and gauge data inputs and merger techniques. The average annual global precipitation rates, calculated from data common in regions/times to both GPCP and CMAP, are similar for the two. However, CMAP is larger than GPCP in the tropics because: (1) CMAP values in the tropics are adjusted month-by-month to atoll gauge data in the West Pacific, which are greater than any satellite observations used; and (2) CMAP is produced from a linear combination of data inputs, which tends to give higher values than the microwave emission estimates alone to which the inputs are adjusted in the GPCP merger over the ocean. The CMAP month-to-month adjustment to the atolls also appears to introduce temporal variations throughout the tropics which are not detected by satellite-only products.

On the other hand, GPCP is larger than CMAP in the high-latitude oceans, where CMAP includes the scattering based microwave estimates which are consistently smaller than the emission estimates used in both techniques. Also, in the polar regions GPCP transitions from the emission microwave estimates to the larger TOVS-based estimates. Finally, in high-latitude land areas GPCP can be significantly larger than CMAP because GPCP attempts to correct the gauge estimates for errors due to wind loss effects.

1. Introduction

One of the goals of the World Climate Research Program is monthly global precipitation datasets for the analysis of climatic variability and the validation of climate models. The Global Precipitation Climatology Project (GPCP) was established in 1986 to address these issues. GPCP has released a community satellite-gauge combined precipitation data set (Huffman et al. 1997) for the period July 1987 through the present, and has extended that data set back to 1979 in an experimental version. A second data set, CPC's merged analysis of precipitation (CMAP) (Xie and Arkin 1997), has also become available. CMAP also extends back to 1979. Xie and Arkin (1997) briefly compared GPCP with their observation-only version of CMAP and showed significant differences over both the tropical and the extratropical oceans. Differences over extratropical land are attributed to the gauge correction used by Huffman et al. (1997) to account for systematic errors due to aerodynamic effects on the gauge estimates. This correction produces higher precipitation rates in regions of snowfall and strong winds in the GPCP analyses.

This study advances the comparison initiated by Xie and Arkin (1997) by diagnosing the data sources and merger techniques that are most important to the differences in precipitation, especially over ocean regions. For the ten-year period 1988-97, the observation-only version of CMAP (CMAP/O) is compared with a preliminary globally complete version of GPCP, which incorporates the inputs described by Huffman et al. (1997) plus estimates derived from the TIROS (Television Infrared

Observation Satellite) Operational Vertical Sounder (TOVS; Susskind et al. 1997) in the extratropics.

2. Data

This section provides a brief description of the data sources used in the GPCP and CMAP mergers detailed in Huffman et al. (1997) and Xie and Arkin (1997). Both data sets adjust to the Global Precipitation Climatology Center's (GPCC) gauge analysis over land (Rudolf et al. 1994), using similar techniques. Huffman et al. (1997) also correct the gauge data for gauge aerodynamic effects (Sevruk 1989) using the Legates and Willmott (1990) climatological corrections. Both data sets include the infrared-based GPI (Arkin and Meisner 1987) and scattering (Grody 1991; Ferraro et al. 1994) and emission (Wilheit et al. 1991) estimates from the Special Sensor Microwave/Imager (SSM/I).

Xie and Arkin (1997) combine the scattering and emission estimates for all data blocks while GPCP chose to use the scattering estimate alone over land, the emission estimates alone over ocean, and a combination in coastal areas (Huffman et al. 1997). In this study precipitation estimates were defined as "ocean data" if the surface of the 2.5 degree grid block was greater than 75% water; otherwise they were categorized as "land data", which is close but not identical to the GPCP land/ocean separation. Two additional data sources in the CMAP merger, the OLR-based Precipitation Index (OPI; Xie and Arkin 1998) and the Microwave Sounding Unit (MSU) (Spencer 1993), allow for the extension of the record back to 1979. The OPI is based on relations of OLR monthly anomalies with pre-OPI CMAP analyses which include gauge data . The GPCP

and CMAP merger techniques are described in Huffman et al. (1997) and Xie and Arkin (1997) and a brief summary regarding ocean data suffices here. For CMAP, the satellite estimates are combined linearly through the maximum likelihood estimation method. Bias is removed in the tropics on a month-to-month basis by comparison with monthly atoll gauge observations in the West Pacific and by subjective extrapolation of the adjustment into the extratropics (Xie and Arkin 1997). The atoll adjustment process produces a mean increase of 9% in the deep tropics.

For GPCP, the microwave estimates are approximately time- and space-matched with geo-IR observations to derive a monthly microwave/IR calibration ratio for each grid box. These are then applied to the full set of GPI estimates from 40° N to 40° S, producing a precipitation field which has the sampling of the IR data and the bias of the microwave estimates (Huffman et al. 1997). This estimate is supplemented with SSM/I poleward of 40°, then combined with gauge over land using inverse-variance weighting (Huffman et al. 1997).

Further development work in GPCP has led to a technique to merge TOVS-based estimates (Susskind et al. 1997), adjusted to the GPCP existing fields, into the GPCP combination scheme for the purpose of filling in missing and uncertain data in the high latitudes. The TOVS-based precipitation estimates are a function of retrieved cloud-top pressure, cloud fraction and water vapor. The TOVS sounding retrieval process uses a first guess based on a general circulation model so there is a potential model influence on retrieved water vapor, and therefore estimated precipitation at high latitudes. However, the model first guess influence is very weak (Susskind, personal

communication), but studies are underway to quantify the model impact on the precipitation estimates.

Finally, a version of CMAP (hereafter CMAP*) and GPCP (hereafter GPCP*) before merger with gauge information over land (GPCP) and before the merger with gauges and adjustment based on atoll gauge data (CMAP) are also used in this study. Essentially these two additional products are "satellite-only" products.

3. Climatologies

The 1988-97 climatologies of GPCP and CMAP derived precipitation are shown in Fig. 1, along with the climatologies of Legates and Willmott (1990) and Jaeger (1976). In all fields tropical convection features such as the Intertropical Convergence Zone (ITCZ) and South Pacific Convergence Zone (SPCZ) stand out. Overall, precipitation rates associated with these systems are higher for CMAP than GPCP, and the locations of the peaks are different for the two data sets. The rainiest point on Earth in the GPCP analysis (9.8 mm/day) is over Borneo at 115° E longitude, while in the CMAP analysis the highest climatological value (11.4 mm/day) is in the SPCZ at 5° S and 160° E. GPCP's maximum precipitation rate in the Pacific ITCZ (9.6 mm day^{-1}) is found in the eastern half (Fig. 1a), while CMAP peaks (10.8 mm day^{-1}) further west (Fig. 1b).

The Legates and Willmott climatology has an eastern Pacific Ocean maximum that is inconsistent with both the GPCP and CMAP maps (Fig. 1a,b). The Jaeger climatology generally agrees with the CMAP and GPCP analyses in the tropics,

although the ITCZ is less continuous across the Pacific ocean, somewhat weaker and a little broader (Fig. 1d).

The extratropical storm tracks extend eastward over a larger area of the North Pacific and Atlantic in GPCP (Fig. 1a) with significantly higher values above 50°N. In the Southern Hemisphere mid-latitudes both analyses show the maxima off the southeast coast of Africa, in the middle of the South Pacific Ocean and off the east coast of South America. The GPCP analysis also has a nearly separate zonal maximum at 55-60°S, similar to the feature in the Jaeger climatology. Both the satellite and conventional (ship) estimates are poor in this area and the existence, shape or strength of this feature is open to question.

The annual cycles of mean precipitation are similar for GPCP and CMAP (see Fig. 15 in Xie and Arkin 1997) and are not discussed here for brevity.

The zonal averages of the CMAP and GPCP estimates, as well as the long-term climatologies of Legates and Willmott (1990) and Jaeger (1976), are shown in Fig. 2, both globally, and ocean only. Precipitation rates are highest in the tropics with a peak between 10° N and the Equator associated with the average position of the ITCZ in the Atlantic and Pacific basins (Fig. 1). Extratropical precipitation is greatest between 40 and 60 ° latitude in the region of the storm tracks (Figs. 1,2). CMAP is larger than GPCP in the tropics, while GPCP exceeds CMAP in the mid- to high-latitudes. The Legates-Willmott climatology is significantly higher than the CMAP estimates in the tropics and comparable to GPCP in the extratropics (Fig. 2). The L-W zonal mean is suspect in the tropics due to the anomalous feature in the Pacific Ocean (Fig. 1d; Janowiak et al. 1995). The Jaeger climatology shows a broader peak in Fig. 2a from 10°

N to the Equator than the other precipitation data sets. The Jaeger precipitation rates are comparable to CMAP in the Northern Hemisphere and GPCP in the Southern Hemisphere (Fig. 2a).

The ocean profile (Fig. 2b) is mostly different from the combined profile in the mid-latitude Northern Hemisphere. North of 45°there is a greater separation among estimates, with the order from lowest to highest estimate being: CMAP, Jaeger, Legates-Willmott, and GPCP (Fig. 2b). The tropical peak differences also become larger when only ocean is considered, with the range increasing to 3 mm/day. The GPCP profile clearly shows a double peak in the Southern Hemisphere mid-latitudes.

In summary, the zonal averages of the four climatologies vary somewhat in magnitude but have similar profiles. One exception is in the Southern Hemisphere where GPCP, Legates-Willmott, and Jaeger all have a broad peak of precipitation from 40° to 60° S and CMAP has a narrower peak between 30° and 40° S (Fig. 2). Reasons for this difference between CMAP and GPCP in the south extratropical oceans will be explored in the next section.

Table 1 quantifies the differences between GPCP, CMAP and the long-term climatologies of Legates-Willmott and Jaeger shown in Figs. 1 and 2. The globally averaged precipitation rates for ocean, land, and all data blocks are about the same for GPCP, CMAP, and Jaeger, while Legates-Willmott is higher. In the tropics the Legates-Willmott climatology is highest and the Jaeger climatology is in the range of the GPCP and CMAP estimates. In the mid-latitudes the Legates-Willmott climatology is

comparable to GPCP while the Jaeger climatology falls between the GPCP and CMAP estimates.

The field of GPCP – CMAP difference (Fig. 3, ref. Fig. 1) is negative over the Indian, West Pacific, and far East Pacific Oceans while positive differences cover much of the high-latitude oceans. The differences in the monthly climatologies (not shown) are similar to Fig. 3. The largest differences are coincident with the highest precipitation rates. Thus, the high latitude winter hemisphere and tropical summer hemisphere have the largest differences.

Some artifacts in the data sets are noted. Fig. 1a (GPCP) shows an isolated block of high rain rates off the northeast coast of Japan and an anomalous tongue of high rain rates in the North Atlantic storm track just to the east of Newfoundland. These show as red dots in the difference map (Fig. 3). CMAP has anomalously high precipitation rates over the Tibetan plateau (Fig. 1b). These artifacts may result from surface ice contamination in the merger techniques, as they are apparent only in the boreal winter season.

Fig. 4 shows precipitation climatologies before the merger of any surface data (GPCP* and CMAP*). Over oceans, the difference map (Fig. 4c) is similar to Fig. 3. However, in the tropics the differences are less pronounced. The eastern vs. western Pacific Ocean differences due to the satellite input are now clearer. In the western Pacific CMAP is still significantly higher than GPCP. However, in the eastern Pacific GPCP is somewhat higher in the regions of high precipitation with lower values than CMAP in surrounding areas. In the Atlantic Ocean ITCZ GPCP generally has the higher values. Focusing on the land, GPCP* is higher than CMAP* over Africa and

South America, while CMAP* is larger than GPCP* over most of the Maritime Continent. The differences over land are smaller in the mid-latitudes.

4. Difference evaluation

In this section data sets used in the mergers are analyzed to uncover reasons for the regional variations between GPCP and CMAP (Figs. 3, 4c). The areas used for comparison are shown in Fig. 3.

In the mid- to high-latitudes (outside 40° latitude) CMAP is produced from a linear combination of SSM/I, OPI, and MSU. Over extratropical oceans GPCP merges TOVS with the lower microwave emission estimates, starting at 40° latitude, and adjusts those estimates to the gauge climatology near the poles. The result is a significant difference between the two analyses over mid- to high latitude oceans (Fig. 3 and Fig. 2). This difference is due to a combination of reasons involving the microwave techniques used and the inclusion of the TOVS-based estimates adjusted to the microwave estimates at 40° latitude and to the land gauge climatology at high latitudes with a linear interpolation of the adjustments at latitudes in between.

Table 2 shows climatological estimates of the input data for case study regions in the high-latitudes along with the CMAP and GPCP totals for that region. In the regions shown the GPCP to CMAP ratio varies, but is often above 1.5. TOVS, used exclusively by GPCP, gives the largest estimates while SSM/I scattering, exclusively used by CMAP, gives the lowest. Another data input to CMAP, OPI (not shown), tends to be

low compared to Legates and Willmott (1990) and Jaeger (1976) (Xie and Arkin, 1998). Since good validation is lacking over the ocean, which analysis is correct is open to question. The GPCP is closer to the two long-term climatologies and perhaps better corresponds to the frequency of precipitation climatology of Petty (1995) in high latitudes which shows a relatively slow decrease in precipitation frequency poleward of the precipitation maximum.

Positive differences are evident over land regions, especially eastern Russia and the maritime continent of Indonesia (Fig. 3), consistent with the findings of Xie and Arkin (1997). The main reason for these differences is that the GPCP gauge data is adjusted to account for climatological wind loss effects while CMAP data is not. This difference is greatest in the case of snow, therefore the effect is largest over high latitudes.

Overall CMAP is higher than GPCP over the tropical oceans (Fig. 3). When CMAP* (i.e., without atoll adjustment) is considered, the difference is smaller or even reverses. The GPCP satellite-only product is identical to the final product over ocean since no atoll data or adjustments are used. Six regions are analyzed in Table 3. The average precipitation rates for the microwave and infrared data used in the merger techniques are shown. For the West Pacific GPI gives the highest climatological value of 8.75 mm day^{-1}. The SSM/I emission value is 8.33 mm day^{-1}, and the scattering and MSU estimates, used only by CMAP products, are the lowest at 7.46 and 7.21 mm day^{-1} respectively. CMAP* is slightly larger than GPCP (6%). Adding the tropical ocean adjustment based on atoll gauge data increases the CMAP* value by 9%. For the SPCZ GPI and SSM/I emission estimates are high, while the scattering value is low. Overall,

the relationship between GPCP and CMAP in the SPCZ resembles that of the West Pacific. In the Indian Ocean the large GPI values produce a large (> 10%) CMAP*-GPCP difference. The CMAP value increases by another 11% after the atoll-based adjustment, producing a very significant 22% difference in the final products.

However, as we move from the western Pacific to the eastern Pacific and even into the Atlantic Ocean the relation between the products changes. In the central Pacific the various estimates converge as there is only a 1 mm day-1 difference between the largest (SSM/I emission) and smallest (GPI) estimates. A mere 4% difference separates the CMAP* and GPCP averages. The atoll adjustment to CMAP* makes the final CMAP value 13% higher than GPCP.

In the East Pacific GPI gives the smallest precipitation rate (4.14 mm day^{-1}) and MSU gives the largest rate (8.36 mm day^{-1}). Here GPCP is over 0.5 mm day^{-1} greater than the CMAP* value, reversing the pattern of product differences found in the western Pacific and Indian Ocean. When the atoll adjustment is applied CMAP is increased to approximately equal the GPCP value. Similar results are found in the ITCZ in the Atlantic Ocean (see Table 3).

The GPI, which measures cloud top brightness, is high compared to the other estimates in areas of deep convection, including the West Pacific and Indian Ocean for most of the year. GPI is lowest when MSU is highest, as in the East Pacific where stratiform clouds prevail over convective systems. Arkin et al. (1989) showed that OLR is well correlated with GPI precipitation and in fact, precipitation rates derived from OLR (Janowiak and Arkin 1991) have been used to fill in spatial gaps in the GPI

(Huffman et al. 1995; Xie and Arkin 1996). An examination of Table 3 suggests that GPI and OPI are closely related in the tropics. The average of SSM/I emission and scattering, GPI, and MSU was found to be lower than the CMAP satellite-only value in the West Pacific, Indian Ocean, and SPCZ, but higher in the East Pacific, indicating that OPI and GPI have about the same impact on the CMAP product.

Over equatorial Africa there is a large difference between the satellite-only products (Fig. 4), with the GPCP* estimate being 9.06 mm day^{-1} and CMAP* giving a value of 6.46 mm day^{-1}. This is in contrast to the similar climatologies of the satellite-gauge mergers (Fig. 3 and Table 3). The GPCP* estimate is driven by the microwave scattering estimate being used to adjust the GPI over land, while the CMAP* also uses OPI data over land and OPI is adjusted to a base product which includes gauge data (Xie and Arkin 1997). Both CMAP and GPCP adjust to the gauges in the final merger.

5. Time variations of tropical precipitation

When examining interannual variations of the geographic distribution of precipitation, such as those related to ENSO, CMAP and GPCP show very similar regional patterns. However, when these variations are integrated over the tropics, differences between the two products emerge. Fig. 5 shows time series plots of CMAP, CMAP*, and GPCP averaged over the tropical (30° N to 30° S) oceans. Here "oceans" refers to grid blocks with 100% ocean surface. Thus, the only difference between CMAP* and CMAP would be attributed to the adjustment applied across the tropical oceans based on the West Pacific atoll data. Interestingly, during 1988-96 GPCP and CMAP* have similar magnitudes (3.0 mm/d and 3.1 mm/d) and follow each other fairly

well, both on short-term variations and on longer-term variations with time scales of a year or two. The general minima centered on late 1989 and late 1995 are simultaneous with La Nina events and the higher values from 1990 through most of 1994 are during a period of generally higher than average SSTs in the central and eastern Pacific Ocean associated with El Nino-like precipitation conditions. CMAP (after the atoll adjustment) is about 10% higher than CMAP* and does not clearly show the long-term variations .

The correlations among the products are given in Table 4. The last column denotes the correlation when the products are integrated over the tropical ocean as in Fig. 5. The two main products, GPCP and CMAP, are essentially uncorrelated with a correlation coefficient of 0.24. However, the correlation between GPCP and CMAP* (i.e., CMAP without the month-by-month atoll adjustment) is relatively high (0.75). The correlation between the two CMAP products is surprisingly low (0.40). In addition, the correlation coefficients between CMAP and the individual satellite estimates before and after the atoll adjustment procedure drop from 0.83 to 0.32 (GPI) and 0.73 to 0.25 (microwave emission).

When the products are examined on a regional scale, all three products are highly intercorrelated (Table 4). On a regional level the variations are dominated by the large amplitude annual cycle and low frequency variations (ENSO). In fact, the highest correlations are found in regions 3 and 4 (Table 4), which are dominated by strong annual and semi-annual cycles respectively. However, when the fields are averaged over the entire tropical ocean, most of the ENSO and seasonal signals are averaged out and the relatively small amplitude signals remaining represent the time variations of integrated, tropical oceanic rainfall. The magnitude of the variation of the atoll

adjustment can be seen from examination of the ratio CMAP/CMAP* averaged over 10° N to 10° S, which varies from 0.90 to 1.27. It thus appears that the atoll adjustment is introducing variations to the final CMAP product that result in a drastic lowering of correlations between it and either CMAP* (and its satellite inputs) and GPCP. In other words this indicates that the two satellite-only products (GPCP and CMAP*) are in better agreement on the month-to-month scale over the ocean than CMAP and CMAP*. Since the magnitude of integrated precipitation is important for computing the strength of the hydrologic cycle, this effect should be examined further.

6. Summary and conclusions

Global observations of precipitation are important for the validation of climate models, understanding of the hydrological cycle, and investigation of extreme events, such as ENSO. The objective of this study was to compare two recent global precipitation products, the Global Precipitation Climatology Project (GPCP) community data set (Huffman et al. 1997) and CPC's merged analysis of precipitation (CMAP) (Xie and Arkin 1997) and understand the reasons for the differences.

The average annual global precipitation rates, calculated in areas common to both GPCP and CMAP, are similar for the two. However differences are apparent regionally, as CMAP is larger than GPCP in much of the tropics (by approximately 10%), especially over the waters surrounding the maritime continent. In contrast, in the mid- to high-latitude oceans GPCP exceeds CMAP.

Over the tropical oceans the differences in the products are ascribed to the different input estimates and to the different methods of removing bias in the two techniques. CMAP in this region is produced from a linear combination of data inputs, and then the resulting combination is adjusted on a month-to-month basis to West Pacific atoll gauges. The GPCP product uses microwave emission estimates to calibrate or adjust the GPI IR estimates and, therefore, has mean values close to the microwave emission estimates. The generally larger CMAP values over the tropical oceans are due to higher satellite inputs (e.g., GPI in the western Pacific and MSU in the eastern Pacific) and the atoll-based adjustment, which is a positive 9% adjustment in the mean.

Applying the atoll adjustment to the entire tropical ocean on a month-to-month basis also affects the CMAP interannual variation of integrated tropical ocean rainfall. The atoll adjustment essentially eliminates the correlation between CMAP and GPCP for this parameter. CMAP does not reproduce the long-term variations in global, tropical ocean totals associated with ENSO that are evident in GPCP and the individual input satellite products. This significant difference between the two products may need further examination.

The data sources used in the precipitation mergers contribute to the differences over the high-latitude oceans. CMAP and GPCP both use emission-based microwave estimates, while CMAP includes the scattering estimates which are consistently smaller. Also, in the high-latitudes GPCP transitions from SSM/I to TOVS-based estimates, which are consistently higher. These two effects lead to a higher estimate in the GPCP product.

Over land, both data sets adjust to the rain gauges in the final stages of production, which accounts for generally good agreement, with GPCP generally slightly higher, because GPCP adjusts the gauge estimates upward for losses due to wind effects. However, in some land regions, in particular Russia during winter, GPCP is significantly higher than CMAP. This is because the adjustment factors are largest in high latitude during winter to account for presumed underestimates of snow.

Observations from the Tropical Rainfall Measurement Mission (TRMM), which includes infrared, passive microwave, and radar instruments, are now being used to evaluate the precipitation estimates in the tropics.

Table Captions:

Table 1. Global, tropical, and extratropical averages of precipitation rates in mm day^{-1}

for GPCP and CMAP (1988-97) and long-term climatologies of Legates-Willmott and

Jaeger. Averages are for ocean, land, and all data.

Table 2. Regional averages of extratropical precipitation rates in mm day^{-1}. Period is

1988 to 1996 for all products except MSU, which is October 1987 to September 1996.

See Fig. 3 for location of boxes in the North Pacific, North Atlantic, South Pacific,

South Atlantic, and South Indian Ocean. At these latitudes TOVS, and SSM/I emission

(e) estimates are used to produce GPCP over ocean. MSU and both SSM/I emission and

scattering (s) estimates are used to produce CMAP over ocean.

Table 3. Regional averages of tropical precipitation rates in mm day^{-1}. Period is 1988 to

1996 for all products except MSU, which is October 1987 to September 1996. See Fig.

3 for location of boxes in the Indian Ocean, West Pacific, South Pacific Convergence

Zone (SPCZ), Central Pacific, East Pacific, and Atlantic Oceans. At these latitudes GPI and SSM/I emission (e) estimates are used to produce GPCP over ocean. GPI, MSU, and both SSM/I emission (e) and scattering (s) estimates are used to produce CMAP* over ocean. CMAP includes the atoll adjustment.

Table 4. Correlation coefficients between CMAP and CMAP*, CMAP and GPCP, and CMAP* and GPCP over oceanic (100% ocean surface) regions in the tropics. R1 (30° N - 30° S; 30° E - 120°E) represents the Indian Ocean, R2 (30° N - 30° S; 120° E - 120°W) the West-central Pacific, R3 (30° N - 30° S; 120° W - 60°W) the East Pacific and Caribbean Sea, R4 (30° N - 30° S; 60° W - 30°E) the Atlantic, and R5 the global tropics.

Figure Captions:

Fig. 1. Precipitation climatologies in mm day^{-1} for (a) GPCP and (b) CMAP during the period 1988-97, and the long-term climatologies of (c) Legates-Willmott and (d) Jaeger.

Fig. 2. Zonally-averaged precipitation rates in mm day^{-1} for GPCP and CMAP during the period 1988-97, and the long-term climatologies of Legates-Willmott and Jaeger. (a) global (b) ocean.

Fig. 3. Difference of GPCP minus CMAP precipitation climatologies in mm day^{-1}. Boxes represent areas where precipitation averages were computed for Tables 2 and 3.

Fig. 4. Precipitation climatologies in mm day^{-1} derived from satellites only. (a) GPCP*, (b) CMAP*, and (c) GPCP* minus CMAP* for the period 1988-96.

Fig. 5. 1988-96 time series of tropical precipitation averaged over grid blocks with 100% ocean surface. Units are in mm day^{-1}. Dashed line is for CMAP, dotted line is for GPCP, and solid line is for CMAP* (without atoll adjustment).

References:

Arkin, P. A. and B. N. Meisner, 1987: The relationship between large-scale convective rainfall and cloud cover over the Western Hemisphere during 1982-84. *Mon. Wea. Rev.*, **115**, 51-74.

_____, A. V. R. K. Rao, and R. R. Kelkar, 1989: Large-scale precipitation and outgoing longwave radiation from INSAT-1B during the 1986 southwest monsoon season. *J. Climate*, **2**, 619-628.

Ferraro, R. R., N. C. Grody, G. F. Marks, 1994: Effects of surface conditions on rain identification using the SSM/I. *Remote Sens. Rev.*, **11**, 195-209.

Grody, N. C., 1991: Classification of snow cover and precipitation using the Special Sensor Microwave Imager (SSM/I). *J. Geophys. Rev.*, **96**, 7423-7435.

Huffman, G. J., R. F. Adler, P. Arkin, A. Chang, R. Ferraro, A. Gruber, J.

Janowiak, A. McNab, B. Rudolf, U. Schneider, 1997: The Global Precipitation Climatology Project (GPCP) combined precipitation dataset. *Bull. Amer. Meteor. Soc.*, **78**, 5-20.

_____, R. F. Adler, B. R. Rudolf, U. Schneider, and P. R. Keehn, 1995: Global precipitation estimates based on a technique for combining satellite-based estimates, rain gauge analysis, and NWP model precipitation information. *J. Climate*, **8**, 1284-1295.

Janowiak, J. E., and P. A. Arkin, 1991: Rainfall variation in the tropics during 1986-1989, as estimated from observations of cloud-top temperature. *J. Geophys. Res.*, **96**, 3359-3373.

_____, J. E., P. A. Arkin, and P. P. Xie, 1995: An examination of the east Pacific ITCZ rainfall distribution. *J. Climate*, 8, 2810-2823.

Jaeger, L., 1976: Monatskarten des Niederschiags fur die ganze Erde. *Berichte des Deutscher Wetterdienstes*, Offenbach, 33 pp. and plates.

Legates, D. R. and C. J. Willmott, 1990: Mean seasonal and spatial variability in gauge corrected global precipitation. *Int. J. Climatol.*, **10**, 111-127.

Petty, G. W., 1995: Frequescies and characteristics of global oceanic precipitation from shipboard present-weather reports. *Bull. Amer. Meteor. Soc.*, **76**, 1593-1616.

Rudolf, B., H. Hauschild, W. Rueth, and U. Schneider, 1994: Terrestrial precipitation analysis: Operational method and required density of point measurements. *NATO ASI Series*, **126**, 173-186.

Sevruk, B., 1989: Reliability of precipitation measurements. *Proc. WMO/IAHS/ETH Workshop on Precipitation Measurements*, St. Moritz, Switzerland, WMO, 13-19.

Spencer, R. W., 1993: Global oceanic precipitation from the MSU during 1979-91 and comparisons to other climatologies. *J. Climate*, **6**, 1301-1326.

Susskind, J., P. Piraino, L. Rokke, L. Iredell, and A. Mehta, 1997: Characteristics of the TOVS pathfinder path A dataset. *Bull. Amer. Meteor. Soc.*, **78**, 1449-1472.

Wilheit, T. J., A. T. C. Chang, and L. S. Chiu, 1991: Retrieval of the monthly rainfall indices from microwave radiometric measurements using probability distribution functions. *J. Atmos. Oceanic Technol.*, **8**, 118-136.

Xie, P., and P. A. Arkin, 1996: Analyses of global monthly precipitation using gauge observations, satellite estimates, and numerical model predictions. *J. Climate*, **9**, 840-858.

_____ and _____, 1997: Global precipitation: a 17-year monthly analysis based on gauge observations, satellite estimates, and numerical model outputs. *Bull. Amer. Meteor. Soc.*, **78**, 2539-2558.

_____ and _____, 1998: Global monthly precipitation estimates from satellite-observed outgoing longwave radiation. *J. Climate*, **11**, 137-164.
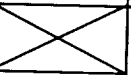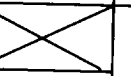
PRECIPITATION RATE (mm day^{-1}) 1988-97				
90N to 90S	GPCP	CMAP	Legates Willmott	Jaeger
OCEAN	3.0	3.0	3.6	3.0
LAND	2.1	1.9	2.3	2.1
TOTAL	2.7	2.6	3.2	2.7
30N to 30S	GPCP	CMAP	Legates Willmott	Jaeger
OCEAN	3.2	3.6	4.0	3.2
LAND	2.9	2.8	3.2	3.1
TOTAL	3.1	3.3	3.8	3.2
30N to 90N 30S to 90S	GPCP	CMAP	Legates Willmott	Jaeger
OCEAN	2.9	2.3	3.0	2.6
LAND	1.4	1.3	1.6	1.4
TOTAL	2.4	1.9	2.5	2.2

High

MIDLATITUDES

REGION	DATA	MERGE	SSM/I e	SSM/I s	TOVS	MSU
N. PAC 170-180 W 52.5-62.5 N	GPCP	2.92	1.51	⨯	3.32	⨯
	CMAP	1.70		0.78		2.27
N. ATL 20-30 W 50-60 N	GPCP	3.84	2.88	⨯	4.29	⨯
	CMAP	3.02		1.72		4.47
S. PAC 130-140 W 50-60 S	GPCP	2.99	1.90	⨯	3.37	⨯
	CMAP	2.02		0.77		2.78
S. ATL 0-10 W 50-60 S	GPCP	3.18	1.72	⨯	3.64	⨯
	CMAP	1.90		0.76		1.47
S. INDIAN 80-90 E 50-60 S	GPCP	3.33	1.81	⨯	3.79	⨯
	CMAP	2.07		0.76		2.38

TROPICS

REGION	DATA	MERGE	SSM/I		GPI	MSU
			e	s		
INDIAN 80-90 E 10S - EQ	GPCP	7.52		✕		✕
	CMAP*	8.47	7.91	6.69	9.96	7.41
	CMAP	9.30				
W. PAC 145-155E EQ-10N	GPCP	8.25		✕		✕
	CMAP*	8.74	8.33	7.46	8.75	7.21
	CMAP	9.57				
SPCZ 165-175 W 15-5 S	GPCP	6.07		✕		✕
	CMAP*	6.41	6.18	5.42	6.64	5.67
	CMAP	6.95				
CENT. PAC 160-170 W 2.5-12.5N	GPCP	6.06		✕		✕
	CMAP*	6.33	6.56	5.59	5.56	7.08
	CMAP	6.87				
E. PAC 125-135W 2.5-12.5N	GPCP	6.38		✕		✕
	CMAP*	5.87	6.75	5.88	4.14	8.36
	CMAP	6.39				
ATLANTIC 22.5-32.5W 2.5-12.5N	GPCP	5.44		✕		✕
	CMAP*	5.15	5.75	4.78	4.07	5.63
	CMAP	5.62				

Table 4. Correlation coefficients among three precipitation products for 4 tropical oceanic regions and the global tropical oceans

	R1	R2	R3	R4	R5
CMAP-CMAP*	0.89	0.82	0.98	0.94	0.40
CMAP-GPCP	0.81	0.76	0.94	0.90	0.24
CMAP*-GPCP	0.90	0.92	0.97	0.90	0.75

GPCP Precip (mm/day) 1988–97 Climatology   0   3   6   9   12+

CMAP Precip (mm/day) 1988–97 Climatology   0   3   6   9   12+

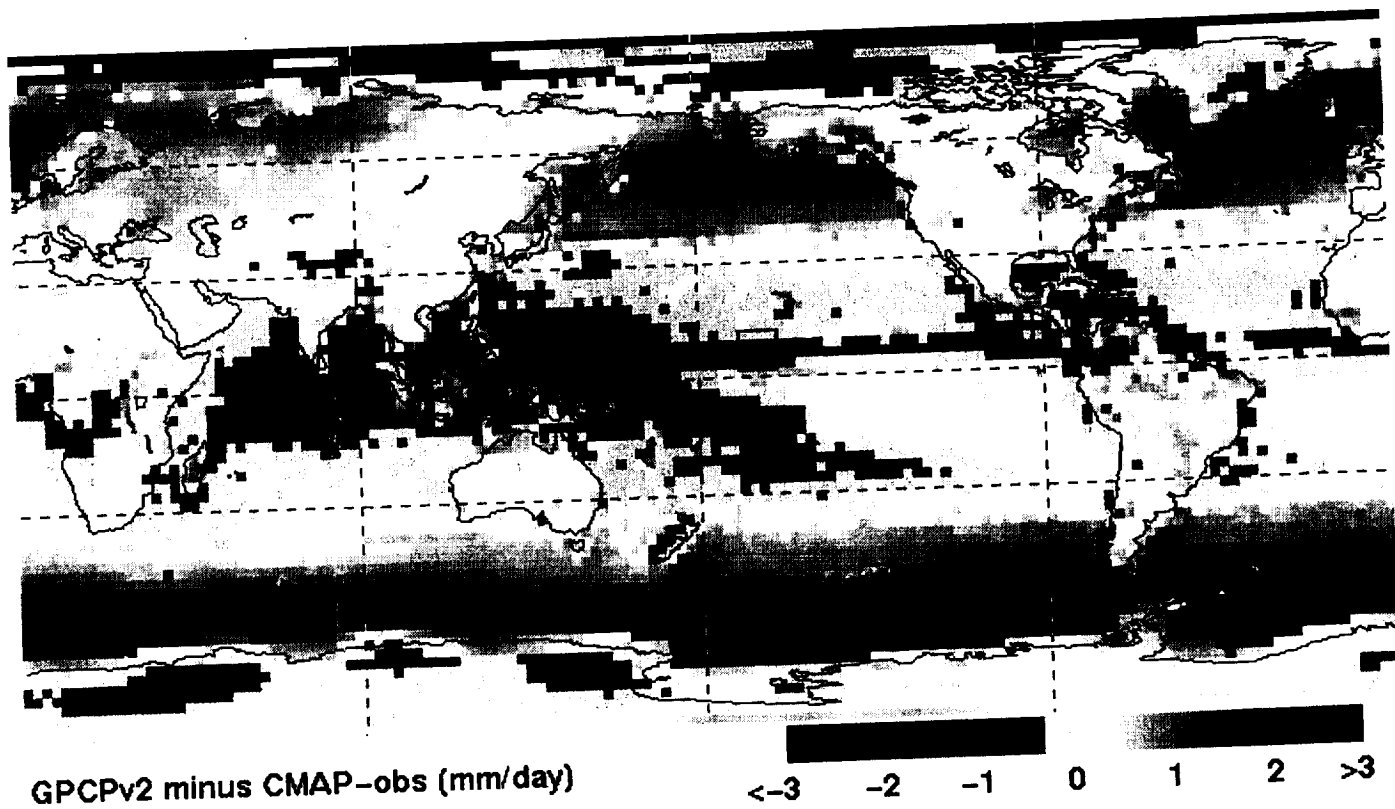Legates Precip (mm/day) Climatology   0   3   6   9   12+

Jaeger Precip (mm/day) Climatology   0   3   6   9   12+

Zonal Mean Precipitation

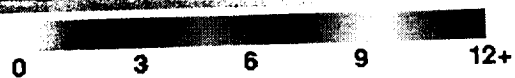## 1988–97 Climatology (a) OCEAN+LAND (b) OCEAN ONLY
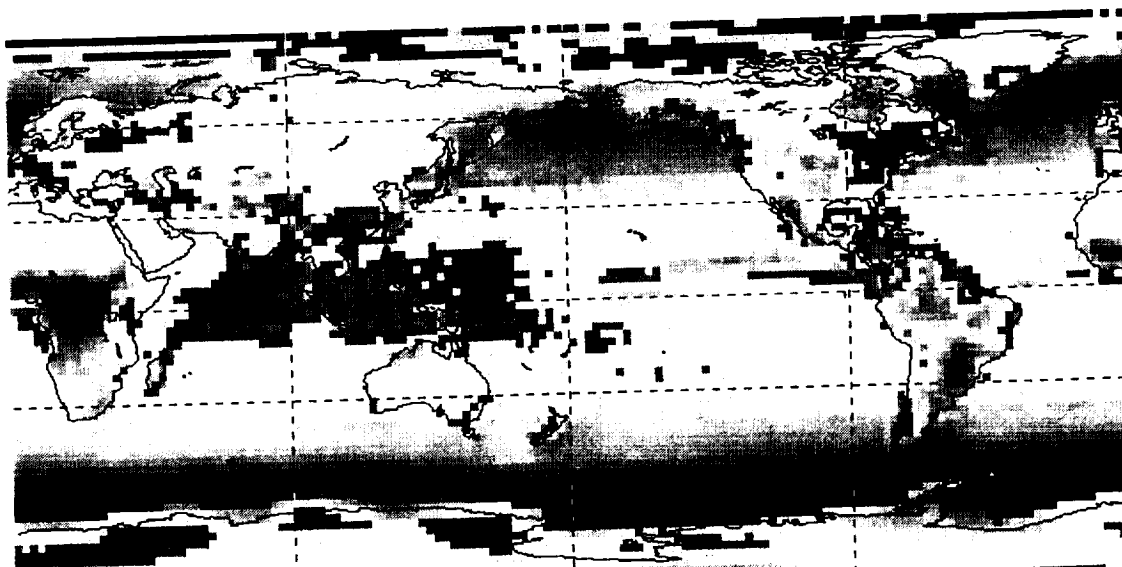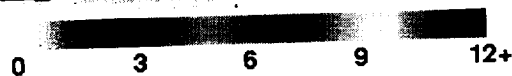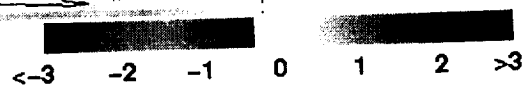
GPCPv2 minus CMAP-obs (mm/day)   <-3   -2   -1   0   1   2   >3
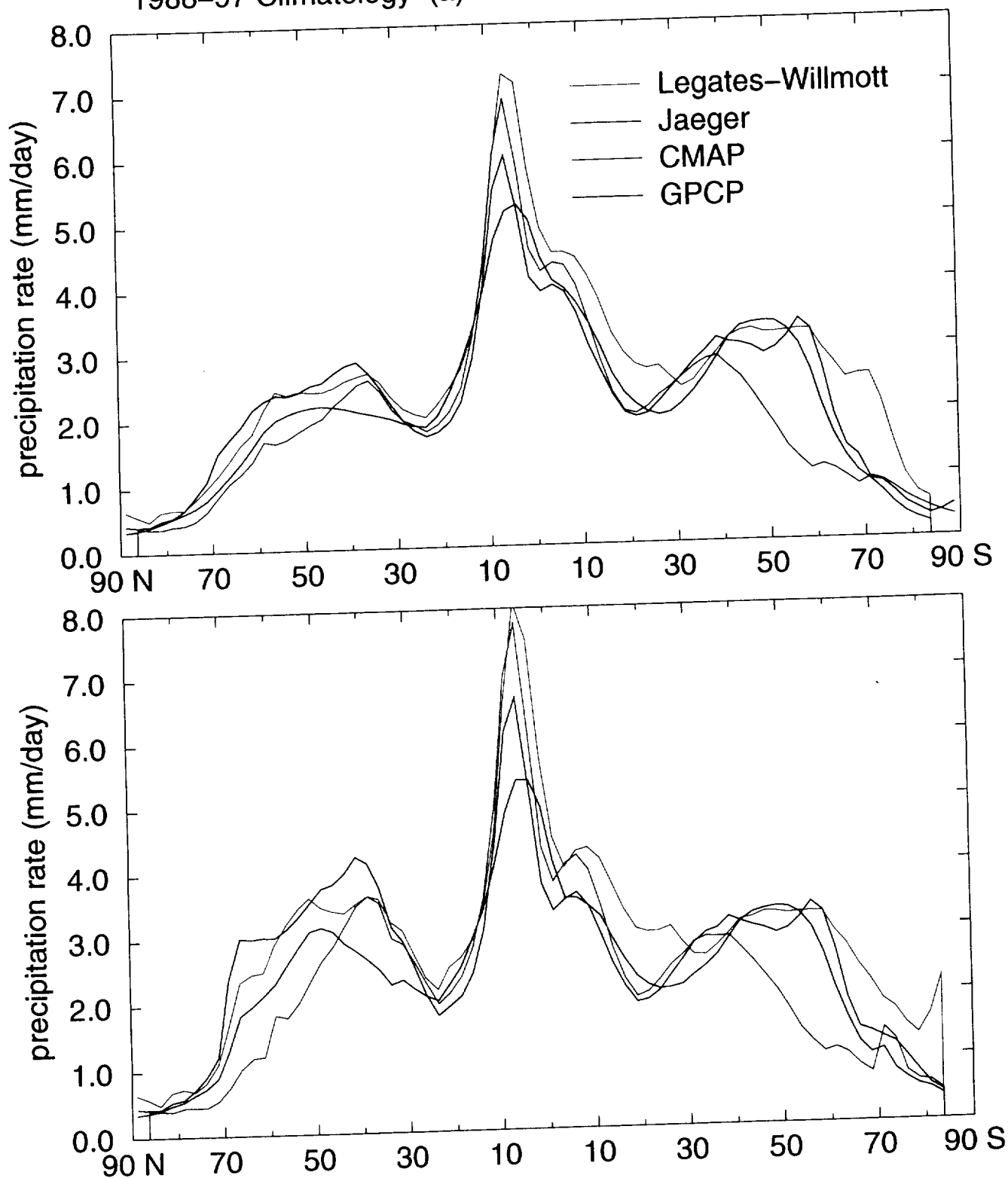
GPCP satellite (mm/day) 1988–96 Climatology   0   3   6   9   12+

CMAP satellite (mm/day) 1988–96 Climatology   0   3   6   9   12+

Difference satellite-only (mm/day)   <–3   –2   –1   0   1   2   >3

precipitation rate (mm/day)
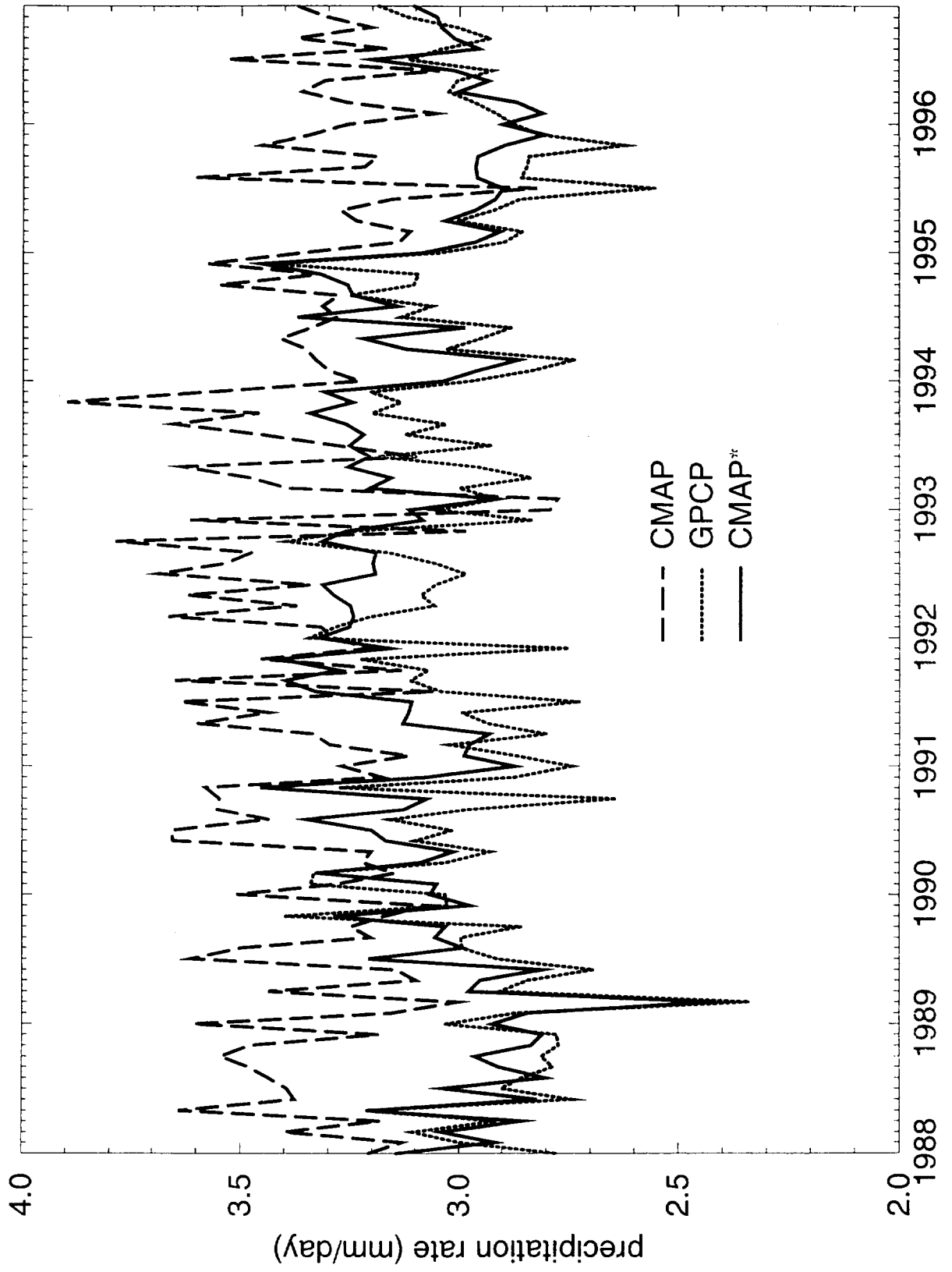
	CMAP	GPCP	CMAP*	MSU	GPI	SSM/I e	SSM/I s
CMAP	1.00	0.24	0.40	0.06	0.32	0.25	0.04
GPCP		1.00	0.75	0.17	0.55	0.96	0.49
CMAP*			1.00	0.32	0.83	0.73	0.36

Comparison of Precipitation Products

100% ocean, 30N – 30S

MSU
GPI
SSM/I e
SSM/I s